A Precise Bandgap Reference with Intrinsic Compensation for Current-Mirror Mismatch

Sizhen Li, Xuecheng Zou, Xiaofei Chen, Zhige Zou, Kai Yu and Hao Zhang*
Department of electronic science and technology
Huazhong University of Science & Technology
Wuhan, P.R.China

***Abstract*—A precise bandgap reference with intrinsic compensation for current-mirror mismatch is presented. In the proposed circuit, the small-signal current variations in the two current paths are self-compensated while in the conventional bandgap core they are multiplied. As a result, error caused by current-mirror mismatch has been much reduced in the proposed circuit. Precise and simple models are developed for error analysis. The complete circuit has also been presented which features simplicity, high accuracy and low power. Based on the 0.6um BiCMOS process technology, the error caused by current-mirror mismatch has been reduced by about 50 times in the proposed bandgap core and the complete circuit achieves a low temperature coefficient of 3.8 ppm/°C and a high power supply rejection ratio (PSRR) of 92db. On typical working conditions, the proposed circuit consumes only a supply current of 3uA.**

I. INTRODUCTION

An ideal Bandgap reference (BGR) should be impervious to variations in process, supply voltage, temperature, load and noise. Much work has been focused on protecting the reference voltage from variations in supply and temperature. However, process variations can decrease the performance of the most well-designed BGR and among various error sources caused by process variations, current-mirror mismatch has been discussed and defined as the leading one [1]. Thus, a bandgap reference with high immunity to current-mirror mismatch is desired.

Fig. 1a shows a widely used BGR with a popular topology---the Brokaw cell.

The bandgap voltage generated can be expressed as

$$\begin{aligned} V_{ref} &= V_{BE(QN2)} + 2V_T\left(\frac{R2}{R1}\right)\ln C \\ &= V_{BE(QN2)} + \frac{2kT}{q}\left(\frac{R2}{R1}\right)\ln C, \end{aligned} \tag{1}$$

where C is the emitter ratio of QN1 over QN2, q is the electron charge, k is the Boltzmann constant and T is the absolute temperature.

Ideally, (1) is obtained under the condition that the collector current through the transistor QN1($I_{C(QN1)}$) and QN2($I_{C(QN2)}$) are identical. However, due to offsetting the input current of the operational amplifier employed and mismatch between R1 and R2, there exits mirror mismatch between $I_{C(QN1)}$ and $I_{C(QN2)}$.

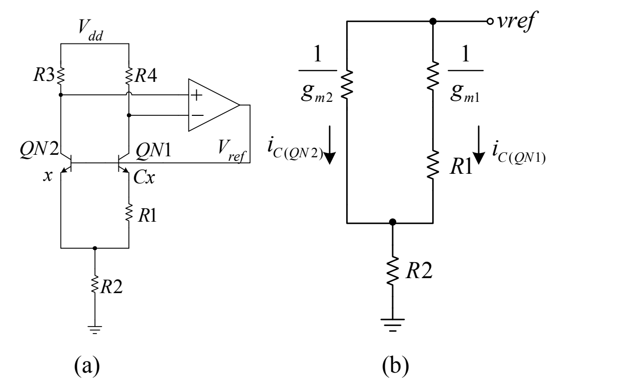

Figure 1. (a) Conventional bandgap reference, (b) Small–signal variation model of the conventional bandgap core

A small-signal variation model is established to discuss the error in reference voltage generated by the current-mirror mismatch which has been defined above. Compared to the traditional method using equations, the small signal method will provide more convenience for analysis.

Fig. 1b illustrates the variation model of the conventional bandgap core described in Fig. 1a. The mirror mismatch between $I_{C(QN1)}$ and $I_{C(QN2)}$ produces small-signal variations of $I_{C(QN1)}$ ($i_{C(QN1)}$) and $I_{C(QN2)}$ ($i_{C(QN2)}$) from their nominal values generated when supposing the currents are well matched. The change in current results in the total variation of the reference voltage (V_{ref}) which can be represented by *vref*.

Assuming there is a δ_M current-mirror mismatch between $I_{C(QN1)}$ and $I_{C(QN2)}$,

$$I_{C(QN2)} = (1+\delta_M)I_{C(QN1)}. \tag{2}$$

the erroneous PTAT current can be represented by I_{PTAT_X} and $i_{C(QN1)}$ is expressed as

$$\begin{aligned} i_{C(QN1)} &= I_{PTAT\_X} - I_{PTAT} \\ &= \frac{V_T \ln[C(1+\delta_M)]}{R1} - \frac{V_T \ln C}{R1} \approx \frac{V_T}{R1}\delta_M. \end{aligned} \tag{3}$$

In Fig. 1b, $g_{m1,2}$ is represented by

$$g_{m1,2} = \frac{\partial I_C}{\partial V_{BE}} = \frac{I_C}{V_T} = \frac{\ln C}{R1} \tag{4}$$

*Contact Author. Email: xfchen@whicc.com

978-1-4244-2342-2/08/$25.00 ©2008 IEEE.

Using the variation model described in Fig. 1b, the overall error in reference voltage can be shown as

$$vref = V_T\delta_M(1+\frac{1}{\ln C}) + V_T\delta_M\frac{R2}{R1}(2+\ln C) \tag{5}$$

It's obvious that the variation of PTAT current through QN1 ($i_{C(QN1)}$) has propagated to *(2+lnC)* $i_{C(QN1)}$ which is the total PTAT current variation and finally results in large error in reference voltage.

As the PTAT slope, *R2/R1lnC*, should be kept constant as about 18, it can be derived that the effect of error caused by current-mirror mismatch can be reduced by decreasing the resistor ratio (*R2/R1*) at the expense of increase in *C*.

Other common techniques for the error minimization are addressed and discussed [2]-[4]. Although the errors have been minimized using the techniques, the voltage reference circuit would become more complex requiring added auxiliary circuit or the area of the layout would become larger.

In this paper, a precise bandgap circuit is presented which features simplicity and low power through internal compensation for current-mirror mismatch.

II. PROPOSED BANDGAP REFERENCE

The basic idea is to have the small-signal collector current of QN1 and QN2 described in Fig. 1a change in the opposite way.

A. Circuit Description

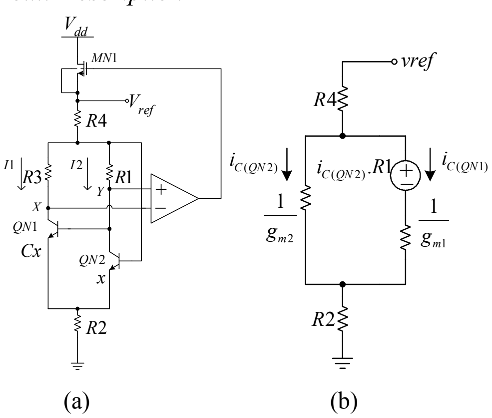

Figure 2. (a) Proposed bandgap reference, (b) Small–signal variation model of the proposed bandgap core.

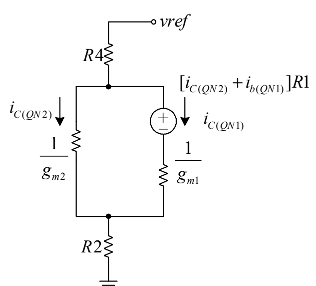

Figure 3. A more precise small–signal variation model of the proposed bandgap core.

The improved bandgap reference is presented in Fig. 2a.The reference voltage is obtained at the top terminal of R4 and is given by the following equation:

$$\begin{aligned} V_{ref} &= V_{BE(QN2)} + \frac{2V_T \ln C}{R1}(R2+R4) \\ &= V_{BE(QN2)} + \frac{2kT\ln C}{qR1}(R2+R4) \end{aligned} \tag{6}$$

Where *C* is the emitter ratio of QN1 over QN2, *q* is the electron charge, *k* is the Boltzmann constant and *T* is the absolute temperature.

B. Variation Model Analysis

Fig. 2b illustrates the variation model of the proposed bandgap core described in Fig. 2a. Assuming there is a δ_M current-mirror mismatch between $I_{C(QN1)}$ and $I_{C(QN2)}$:

$$I_{C(QN2)} = (1+\delta_M)I_{C(QN1)}, \tag{7}$$

Using the same method given in introduction, $i_{C(QN2)}$ is expressed as

$$i_{C(QN2)} = I_{PTAT\_X} - I_{PTAT} \approx \frac{V_T}{R1}\delta_M. \tag{8}$$

In Fig. 2b, $g_{m1,2}$ is represented by

$$g_{m1,2} = \frac{\partial I_C}{\partial V_{BE}} = \frac{I_C}{V_T} = \frac{\ln C}{R1}. \tag{9}$$

and

$$i_{C(QN1)} \approx (1-\ln C)i_{C(QN2)}. \tag{10}$$

vref can be derived from Fig. 2b as

$$vref = \frac{V_T\delta_M}{\ln C} + \frac{V_T\delta_M}{R1}(R2+R4)(2-\ln C). \tag{11}$$

It's obvious that for the case that *lnC*>1, the small-signal current of QN1 and QN2 described in Fig. 2a change in the opposite way which results in the minimization of the total PTAT current variation.

It can be derived from (11) that when

$$\frac{1}{\ln C} + \frac{1}{R1}(R2+R4)(2-\ln C) = 0, \tag{12}$$

vref equals to zero. Solving (12), it was obtained that

$$\ln C = \frac{2x+1}{x} \approx 2 \tag{13}$$

where *x*, *(R2+R4)lnC/R1* is a process dependent constant which is about 18.

In practical design, it's common to choose *C*=8 or *C*=24 for increasing the matching of Bipolar transistor. Thus, we choose *C*=8 for meeting the requirement described in (13).

In the above analysis, the base current of QN1 which is one part of the current passing through R1 is neglected. However, in practical circuit, it's necessary to consider the effect of the base current of QN1. This is due to the fact that the two terms in (11) are close to each other. Thus, a more precise variation model of the proposed bandgap core is presented in Fig. 3, considering the effect of the base current of QN1.

We Suppose

$$i_{b(QN1)} = \frac{1}{\beta 1}i_{C(QN1)}, \tag{14}$$

where *β1* depends on the operating conditions of the transistor, such as temperature and transistor collector current [5]. $i_{C(QN1)}$ can be derived from Fig. 3 as

$$i_{C(QN1)} \approx \frac{1-\ln C}{1+\frac{\ln C}{\beta 1}}i_{C(QN2)}, \tag{15}$$

and results in

$$vref = \left(1 + \frac{1-\ln C}{1+\frac{\ln C}{\beta 1}}\right) i_{C(QN2)}(R2+R4) + \frac{i_{C(QN2)}}{g_{m2}}. \quad (16)$$

Substitute (8) and (9) into (16),

$$vref = \left(1 - \frac{\ln C - 1}{1+\frac{\ln C}{\beta 1}}\right) \frac{V_T \delta_M}{R1}(R2+R4) + \frac{V_T \delta_M}{\ln C}. \quad (17)$$

By comparing between (5) and (17), it is shown that the dominant term $V_T\delta_M(2+lnC)R2/R1$ in (5) is eliminated. The maxim *vref* in (17) is about $V_T\delta_M$/lnC. Thus, the variation in V_{ref} generated by current-mirror mismatch has been much reduced in the proposed bandgap core.

C. Model Simulations

Simulation has been carried out using a 0.6um BiCMOS process technology. The simulation was performed following the schematic in Fig. 1a and Fig. 2a by assuming an ideal OPAmp that, without any load, had an intrinsic gain, of 60db, an output impedance, Rout, of 1kΩ.

Design parameters of the circuit described in Fig. 1a and Fig. 2a are shown in Table I and Tab II. The current-mirror mismatch was simulated by making the value of R4 $(1+\delta_M)$ times that of R3 in Fig. 1a while the mismatch of the same ratio was applied between the value of R3 and R1 in Fig. 2a. A typical mismatch, δ_M of 1% was assumed [6]. Fig. 4 shows the comparison of the simulated and analytical *vref* derived from the conventional and the proposed bandgap core. The analytical error is derived through (5) (11) and (17). It is noteworthy that the parameters of both the two circuits are chosen to reveal the best operating point of the BGR, value for which V_{ref} exhibits the best temperature drift performance.

The results in Fig. 4a show that the variation model described in Fig. 1b provides a simple and good approximation for error analysis. In Fig. 4b and Fig. 4c, a relative error is observed between the simulation and analysis due to the fact that $i_{C(QN1)}$ and $i_{C(QN2)}$ are very close to each other, it is difficult to predict the difference between them. However, by comparing Fig. 4b and Fig. 4c, it is apparent that the model described in Fig. 3 provides much more precise approximation. It also demonstrates that the effect of $\beta 1$ should not be neglected. The simulation results given in Fig. 4c show that under the 0.6um BiCMOS technology used for simulation and under the low collector current level, error caused by current-mirror mismatch in the proposed BGR core is dominated by the second term in (11). Even in the case, the variation of the reference voltage has been largely reduced by about 50 times in the proposed circuit at room temperature and as the temperature rises, error becomes less due to the increasing value of $\beta 1$. Simulation results in Fig. 5a and Fig. 5b demonstrate that in the proposed bandgap core, the current variations in the two current paths are self-compensated while in the conventional bandgap core, they are multiplied.

TABLE I. KEY COMPONENTS IN THE CONVENTIONAL BGR

Components	Value
$I_{C(QN1)}$	0.8uA
$I_{C(QN2)}$	0.8uA
R2	362K
R1	66K
$A_{(QN1)}/A_{(QN2)}$	8

TABLE II. KEY COMPONENTS IN THE PROPOSED BGR

Components	Value
$I_{C(QN1)}$	0.8uA
$I_{C(QN2)}$	0.8uA
R1	66K
R2	10K
R3	66K
R4	352K
$A_{(QN1)}/A_{(QN2)}$	8

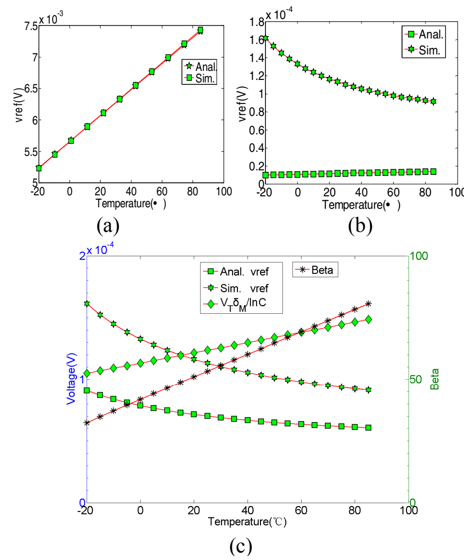

Figure 4. Comparision of simulated and analytical *vref* of (a) conventional BGR, (b) the proposed BGR with the model described in Fig. 2b for analysis, and (c) the proposed BGR with the model described in Fig. 3 for analysis.

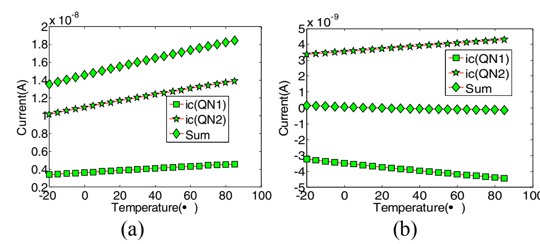

Figure 5. Comparision of simulated current variations of (a) conventional BGR, and (b) the proposed BGR.

III. COMPLETE CIRCUIT AND SIMULATION RESULTS

A. Complete Schematic Circuit Design

Fig. 6 shows the complete schematic circuit of the proposed BGR. The simple amplifier is made up of MP1-3, MN1-3, QN3, QN4 and R5. The transistor MN1 and MP4 provide the current of the BGR. The current provided by MP4 is a constant start-up current for bandgap core.

Based on the consideration of minimizing error sources, choosing devices with good matching characteristics is important in circuit design. In the above circuit, the current-mirror mismatch error would be a function of the resistor value of R1 and R3, the input offset voltage and offset current of the operational amplifier. As a result, for amplifier, we choose basic bipolar input stage built with bipolar transistors with a number of advantages: simplicity, low offset voltage as low as 10uv, low offset drift as low as 0.1uv/°C, well-matched bias current in the inverting and non-inverting inputs. The self-bias active load composed of MP1-3 and MN1-3 is applied to improve the open-loop gain of the amplifier [7].

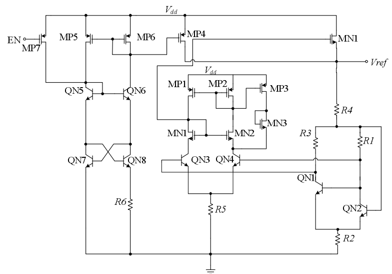

Figure 6. Complete schematic circuit of the BGR.

B. Simulated Performance

The circuit has been simulated in 0.6um BCD process under different temperature and supply voltage conditions with HSPICE. Fig. 7a shows the temperature dependence of the reference voltage. The PSRR performance at room temperature is given in curve of Fig. 7b.

The results show that the proposed circuit generates an output reference voltage with a power supply rejection ratio of 92dB.This is a relative high PSRR due to the fact that the open loop gain of the amplifier in the BGR is 82 db and the supply voltage directly affects the output of the amplifier [8]. Fig. 8 presents the simulated $I_{C(QN1)}$ and $I_{C(QN2)}$ as a function of the supply voltage . The result shows that the small-signal current variations in the two current paths are self-compensated which is the essential reason for the high intrinsic accuracy of the proposed circuit. Higher PSRR may be achieved using some PSRR boosting techniques at the expense of more power consumption and larger area of the circuit.

With the power supply 3V and temperature range from -25°C to 85°C, the temperature coefficient of the reference voltage is only 3.8ppm/°C. On typical working conditions, the proposed circuit consumes only a supply current of 3uA.The simulation results show that the reference has high intrinsic precision.

Table III shows that the current-mirror mismatch caused the error in the output reference and the error in conventional BGR is up to 6.2 mV while that in the proposed is only 0.13mV at room temperature. The relative accuracy is increased by about 50 times.

IV. CONCLUSION

By having the current in the two current paths of BGR change oppositely, a precise bandgap reference with intrinsic compensation for current-mirror mismatch is proposed. Based on the variation model analysis, the area ratio of the two transistors in BGR is chosen to 8 such that the error caused by the current-mirror mismatch can be largely reduced which has been discussed and verified through simulation. A complete circuit applying the proposed BGR structure is simulated which realizes high accuracy over temperature and power supply voltage. On typical working conditions, the proposed circuit consumes only a supply current of 3uA.

TABLE III. SIMULATED ERRORS

Error	Conventional BGR	Proposed BGR
Current-mirror mimatch	1%	1%
Variation in V_{ref}	6.1mV	0.13 mV

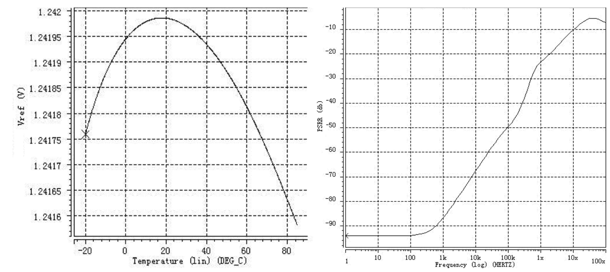

(a) (b)

Figure 7. (a) Temperature dependence of the BGR, (b) PSRR of the BGR.

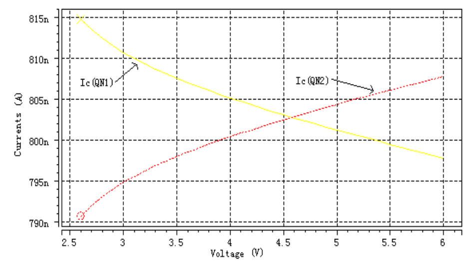

Figure 8. $I_{C(QN1)}$ and $I_{C(QN2)}$ at different supply voltage

REFERENCES

[1] Drennan, P.G., McAndrew, C.C, "Understanding MOSFET mismatch for analog design," IEEE Journal of Solid-State Circuits, 38(3), pp. 450-456, 2003.

[2] GABRIEL A. RINCÓN-MORA, Voltage References, From Diodes to Precision High-Order Bandgap Circuits. IEEE Press, Georgia, 2002, pp. 108-116.

[3] Brito, J.P.M., Klimach, H., Bampi, S., "A design methodology for matching improvement in bandgap references," Quality Electronic Design. ISQED. The 8th International Symposium, pp. 586 – 594, 2007.

[4] Strik, S., "Bandgap voltage reference: errors and techniques for their minimization," Baltic Electronics Conference, pp. 1 – 4, 2006.

[5] Paul R. Gray, Paul J. Hurst, Stephen H. Lewis and Robert G. Meyer, Analysis and Design of Analog Integrated Circuits. Wiley Press, 2001,pp. 23-26.

[6] Gupta, V., Rincon-Mora, G.A., "Predicting and designing for the impact of process variations and mismatch on the trim range and yield of bandgap references," Quality of Electronic Design. ISQED. Sixth International Symposium, pp. 503 – 508, 2005.

[7] Paul R. Gray, Paul J. Hurst, Stephen H. Lewis and Robert G. Meyer, Analysis and Design of Analog Integrated Circuits. Wiley Press, 2001,pp. 278-293.

[8] Giustolisi, G., Palumbo, G, "A detailed analysis of power-supply noise attenuation in bandgap voltage references," Circuits and Systems I: Fundamental Theory and Applications, IEEE Transactions, 50(2), pp. 185 – 197, 2003.